Solar-Terrestrial Physics, 2018. Vol. 4. Iss. 2, pp. 69–72, DOI: 10.12737/stp-41201811. © 2018 V.I. Sivtseva, P.P. Ammosov, G.A. Gavrilyeva, I.I. Koltovskoi, A.M. Ammosova. Published by INFRA-M Academic Publishing House
Original Russian version: V.I. Sivtseva, P.P. Ammosov, G.A. Gavrilyeva, I.I. Koltovskoi, A.M. Ammosova, published in Solnechno-zemnaya fizika, 2018, vol. 4, iss. 2, pp. 109–115,
DOI: 10.12737/szf-41201811 © 2018 INFRA-M Academic Publishing House (Nauchno-Izdatelskii Tsentr INFRA-M)

COMPARISON BETWEEN SEASONAL VARIATIONS IN TIDAL AND INTERNAL GRAVITY WAVE ACTIVITY AS DERIVED FROM OBSERVATIONS AT MAIMAGA AND TIKSI

V.I. Sivtseva
Yu.G. Shafer Institute of Cosmophysical Research and Aeronomy SB RAS, Yakutsk, Russia, verasivtseva@gmail.com

P.P. Ammosov
Yu.G. Shafer Institute of Cosmophysical Research and Aeronomy SB RAS, Yakutsk, Russia, ammosov@ikfia.ysn.ru

G.A. Gavrilyeva
Yu.G. Shafer Institute of Cosmophysical Research and Aeronomy SB RAS, Yakutsk, Russia, gagavrilyeva@mail.ru

I.I. Koltovskoi
Yu.G. Shafer Institute of Cosmophysical Research and Aeronomy SB RAS, Yakutsk, Russia, koltigor@mail.ru

A.M. Ammosova
Yu.G. Shafer Institute of Cosmophysical Research and Aeronomy SB RAS, Yakutsk, Russia, ammosovaam@mail.ru

Abstract. Since 2015, simultaneous observations of temperature of the high-latitude mesopause (87 km) have been made at Maimaga (63.04° N, 129.51° E) and Tiksi (71.58° N, 128.77° E) stations. These stations record spectra with Shamrock (Andor) photosensitive infrared spectrographs detecting the OH (3, 1) band in the near-infrared region (about 1.5 μm). We analyze temperature data obtained in observation seasons from 2015 to 2017. Standard deviations of temperature σ from its mean values are taken as characteristics of wave activity at night. We have obtained standard temperature deviations corresponding to internal gravity waves (IGW) (σ_{gw}) and tidal waves (σ_{td}). Mean night rotational temperatures of hydroxyl emission almost coincide, and seasonal variations of gravity and tidal waves have a similar form during two seasons of simultaneous observations at Tiksi and Maimaga.

Keywords: high-latitude mesopause, hydroxyl emission, internal gravity waves, tidal waves.

INTRODUCTION

The mesopause as a boundary region (80–100 km) between the mesosphere and the thermosphere, where the atmospheric temperature is minimum, has aroused increasing interest in its study. This is due to the fact that the mesopause region actively interacts with solar radiation coming from above and with a broad spectrum of waves propagating upward from the lower atmospheric layers [Brasseur, Solomon, 1987].

Wave activity contributes significantly to the mesopause temperature regime. Tidal waves cause adiabatic compression and expansion of the mesopause region, thus heating or cooling the environment [Chapman, Lindzen, 1972; Brasseur, Solomon, 1987]. IGW propagating upward from the lower atmospheric layers transfer momentum and energy to the mesosphere and thermosphere. In the mesopause region due to wind shift, IGW are subjected to spectral filtering and are absorbed, thus causing heating in this region [Hines, 1974]. Amplitudes of IGW and tidal waves increase with height due to the atmospheric density reduction; thereby the waves can be detected in the upper atmosphere.

In the mesosphere and lower thermosphere, wave activity is studied using both a satellite measurement method and ground-based observations. The most common and accessible ground-based methods are spectral observations of OH (3, 1) emissions, excited in the mesopause region. Numerous rocket measurements have revealed that the emission layer is located at a height of ~87 km and has a halfwidth of ~9 km [Baker, Stair, 1988]. The height of the emitting layer can, however, vary depending on season and wave propagation through the layer [Takano et al., 1990; Yee et al., 1997; Zhang, Shepherd, 1999]. The rotational temperature determined from the distribution of intensities in the hydroxyl band is close to the kinetic temperature of neutral gas at an emission height [Shefov et al., 2006; Noll et al., 2015]. Nowadays this method is widely applied to observations made at the International Network for the Detection of Mesopause Change (NDMC).

Many studies of wave activity in the mesopause region from hydroxyl emission observations have been conducted at midlatitudes [Offermann et al., 2011; Perminov et al. 2013; Perminov et al., 2014]. At the same time there is a lack of such studies at high latitudes. Therefore, of great interest is the temperature behavior and wave activity at the high-latitude mesopause. This paper studies temperature and its standard deviations σ from mean night values in the mesopause region, using measurements made at the high-latitude stations Maimaga (63.04° N, 129.51° E) and Tiksi (71.58° N, 128.77° E).

INSTRUMENTS AND DATA PROCESSING METHOD

To detect the OH (3, 1) band, we employ the photosensitive infrared spectrograph Shamrock SR-303i with an operating wavelength range 1490–1544 nm (manufactured by Andor Technology Ltd), equipped with a high-sensitive infrared iDus InGaAs photodiode detector DU490A-1.7. The spectrograph is of Czerny–Turner design, its focal length is 303 mm, resolution with the effective width of the 0.2 mm entrance slit is 0.8 nm, the aspect angle is ~14°. The Shamrock SR-303i spectrograph is a special-purpose and reliable platform designed for detection of weak light signals in the near-infrared region.

Two identical spectrographs of this type are installed at Maimaga (150 km northward of Yakutsk) and Tiksi stations. At Maimaga, the instrument was put into operational use on January 17, 2013; at the high-latitude station Tiksi, on September 3, 2015. For mutual calibration of these instruments, we made simultaneous observations at Maimaga on August 5–15, 2015. The software we have developed allows the device to work completely offline.

The spectrographs detect the OH (3, 1) band in the near-infrared region (about 1.5 μm) at a >9° angle of dip of the Sun. Detection of this band is advantageous because in this spectral region the auroral emission is much less intense, and the contribution of stray light from the Moon and stars decreases substantially in proportion to $1/\lambda^4$ [Shefov et al., 2006]. This region also exhibits the highest hydroxyl emission intensity. The working cooling temperature of chamber of the spectrographs is set to –50° C to eliminate the temperature drift of the dark current and to reduce it. In these conditions, the spectrographs measure the mesopause temperature with an error of ~2 K (the error was calculated for each measurement separately).

The exposure period for obtaining one measurement of the hydroxyl spectrum in the OH (3, 1) band is 60 s. The short exposure is not only significantly expands the range of periods of IGW under study, but also includes acoustic waves (3–5 min periods) in the spectrum considered. To exclude the acoustic waves from consideration, we average the data in increments of 3 min.

The method of estimating the rotational molecular emission temperature is based on the fitting of the model spectra, constructed with regard to the instrument functions of the device for different predetermined temperatures, to the actually measured spectrum [Ammosov, Gavrilyeva, 2000; Gavrilyeva, Ammosov, 2002]. The OH (3, 1) band is thermalized quite well, and the rotational temperature determined from the band is close to the kinetic temperature of the ambient neutral atmosphere at a height of its emission. To measure the rotational temperature from the hydroxyl band, we use transition probabilities calculated by Mies [1974]. The currently available data on probabilities [van der Loo, Groenenboom, 2007; Goldman et al., 1998] allow us to measure the absolute temperature more precisely. However, we are interested in relative temperature variations, not in its absolute values. Accordingly, for the results to be uniform and to compare them with the results from other studies on wave activity (e.g., Offermann et al., 2011), we apply the transition probabilities obtained by Mies [1974]. Furthermore, Einstein coefficients for low-lying transitions of OH (3, 1) in different data on probabilities differ slightly [Offermann et al., 2010].

To exclude data with a high level of noise interference, we select spectra satisfying the signal/noise ratio of >20 and then average the temperature in increments of 3 min. As a characteristic of night wave activity we take the standard deviation σ of temperature T_i from its mean night value $\bar{T}$:

$$\sigma = \sqrt{\frac{1}{n}\sum_{i=1}^{n}\left(T_i - \bar{T}\right)^2},$$

where n is the number of measured values at nighttime.

This standard deviation is a superposition of different waves, active at nighttime, and the dark-current noise of the detector. According to Offermann et al. [2009], the superposition of waves can be represented as

$$\sigma = \sqrt{\sigma_{\text{td}}^2 + \sigma_{\text{gw}}^2 + \sigma_{\text{noise}}^2},$$

where σ_{td}, σ_{gw}, σ_{noise} are the standard temperature deviations caused by tidal waves, IGW, and dark-current noise of the detector respectively; σ_{noise} was calculated as an arithmetic mean of error of each individual measurement per night. Planetary waves are excluded from consideration because their time scale is much larger than one night.

The σ_{td} value is determined by separating the harmonics corresponding to 24, 12, and 8 hr diurnal tide components from the night temperature series by the method of least squares.

$$f_{\text{td}} = \bar{T} + A_1 \cos\left(\frac{2\pi}{1440}\left(t - \varphi_1\right)\right) + A_2 \cos\left(\frac{2\pi}{720}\left(t - \varphi_2\right)\right) + A_3 \cos\left(\frac{2\pi}{480}\left(t - \varphi_3\right)\right),$$

where f_{td} is the sum of diurnal tide harmonics (periods are given in minutes); A_1, A_2, A_3 are the amplitudes of diurnal tide harmonics; φ_1, φ_2, φ_3 are the harmonic phase shifts; t is the time in minutes.

The result of subtracting the sum of diurnal tide harmonics from the night temperature series corresponds to the contribution of the dark-current noise and IGW propagation to the temperature. Hence, knowing the value of σ_{noise}, we can calculate the standard deviation σ_{gw}.

OBSERVATIONS AND THEIR ANALYSIS

Simultaneous observations with the Shamrock spectrographs at Tiksi and Maimaga were made during two full seasons from 2015 to 2017. Figure 1 shows mean night rotational hydroxyl temperatures derived from observations at these stations. The mean night temperatures obtained in the two seasons of simultaneous observations from 2015 to 2017 closely coincide.

The tidal components of the standard temperature

deviations are shown in Figure 2. The black and red lines indicate moving averages with a 30 day averaging window and represent the seasonal variation in the tidal component σ_{td} for Maimaga and Tiksi respectively.

Values and seasonal variation of the tidal component are roughly the same for both the stations. The seasonal variation in the tidal component of standard temperature deviations σ_{td} varied from 2.5 to 5 K during all the observation seasons.

The standard temperature deviations corresponding to IGW are shown in Figure 3, where lines indicate moving averages with a 30 day averaging window, representing the seasonal variation of the gravitational component σ_{gw}. Values of σ_{gw} are roughly the same for the two observation seasons made at Tiksi and Maimaga in 2015–2017. The seasonal variation in the IGW component varies from 2 to 6.5 K.

When comparing Figures 1 and 3, we can see that the seasonal variation in the IGW component of standard temperature deviations (Figure 3) corresponds visually to that of the mean night temperature (Figure 1). For further analysis, we examine relative values of the standard deviations, i.e. ratios of gravitational and tidal components to mean night temperature ($\sigma_{gw}/\overline{T}$ and $\sigma_{td}/\overline{T}$). This allows us to properly compare the standard deviations for high temperature variations throughout the year. Relative values of the standard temperature deviations are shown in Figures 4 and 5, which also display similar values of tidal and IGW components of standard temperature deviations obtained at Maimaga and Tiksi during the two seasons of simultaneous observations.

In the mid-latitude region, the hydroxyl emission was observed at Wuppertal (51° N, 7° E), Zvenigorod (55.7° N, 36.8° E), and Tory (52° N, 103° E) stations. The comparison of the average standard temperature deviations (σ_N), obtained at Wuppertal ([Offermann et al., 2011], Figure 10), with data on $\left(\sigma_{dd}/\overline{T}\right)$ from Tory ([Perminov et al., 2014], Figure 5, *a*), reveals that seasonal variations (shapes) in summer and autumn months are similar. In particular, the peak of the standard temperature deviations is the same in September (240–270 days of the year).

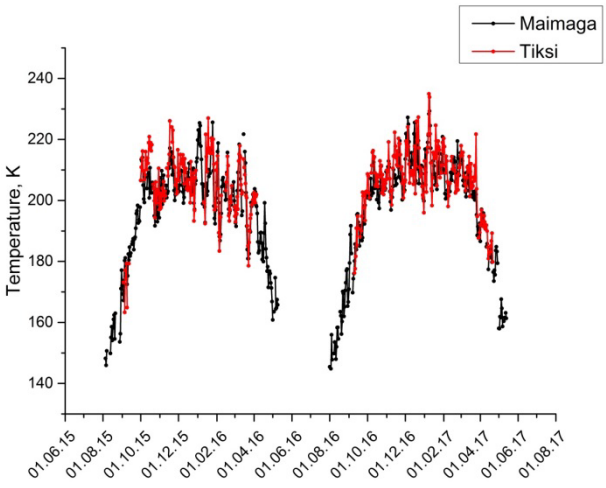

Figure 1. Average night rotational hydroxyl temperatures from observations at Maimaga and Tiksi in 2015–2017

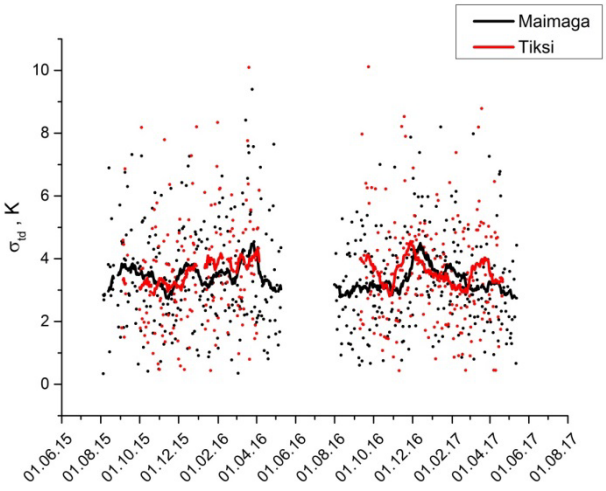

Figure 2. Seasonal variations in the tidal component of standard temperature deviations as a moving average with a 30 day averaging window. The measurements made at Maimaga and Tiksi are highlighted in red and black respectively.

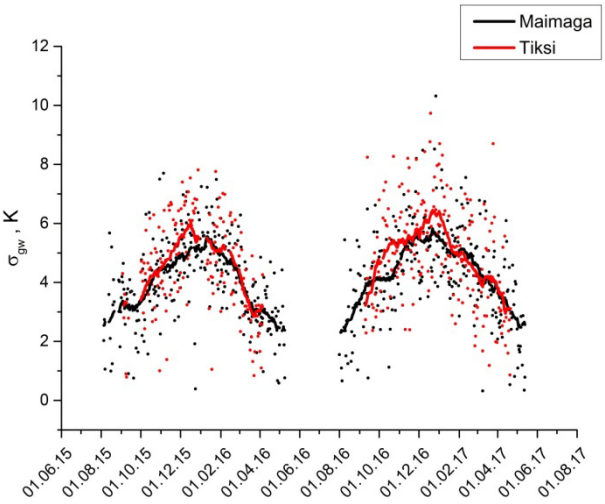

Figure 3. Seasonal variations in the IGW component of standard temperature deviations as a moving average with a 30 day averaging window. The measurements made at Maimaga and Tiksi are highlighted in red and black respectively

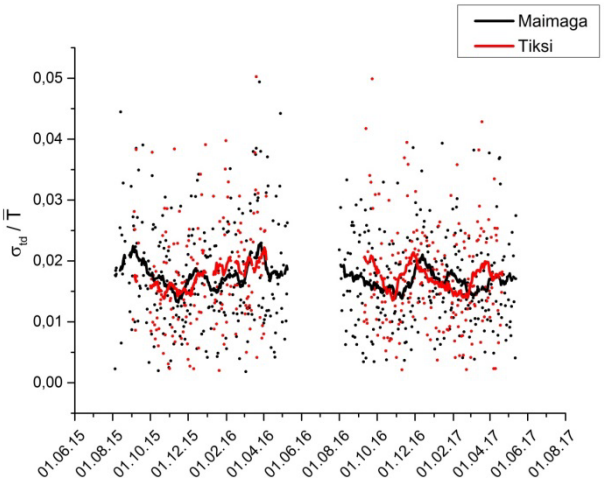

Figure 4. Relative standard temperature deviations caused by tides. The measurements made at Maimaga and Tiksi are highlighted in red and black respectively

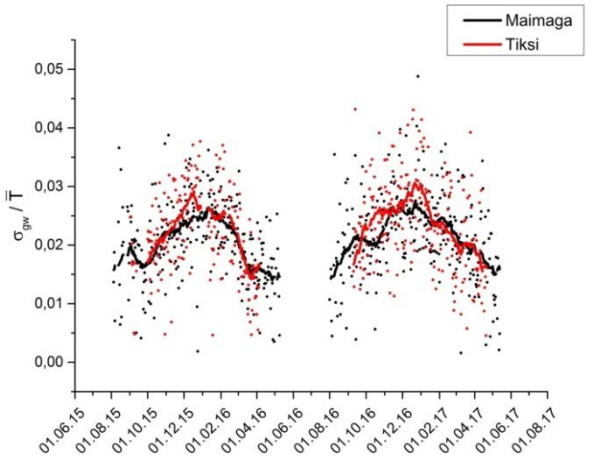

Figure 5. Relative standard temperature deviations caused by IGW. The measurements made at Maimaga and Tiksi are highlighted in red and black respectively

The standard temperature deviations $\sigma_{gw}/\overline{T}$ obtained at Zvenigorod ([Perminov et al.,2014], Figure 5, *c*) and at Maimaga and Tiksi (Figure 5) have a smoother seasonal variation. Values of $\sigma_{gw}/\overline{T}$ in Yakutia are about two times higher than those in Zvenigorod and, except for the peak in September, at Tory. This may be due to the fact that the exposures used to record OH spectra at Zvenigorod and Tory are long (10 min), and hence only waves with periods longer than 30 min can be detected. In this paper, we analyze temperature data with 3 min averaging, which allows us to detect the spectrum of waves with periods of 6 min and more at nighttime.

The relative tidal components of standard temperature deviations $\sigma_{td}/\overline{T}$, obtained at Zvenigorod, Tory, Maimaga, and Tiksi are very close in value.

CONCLUSION

We have studied standard temperature deviations σ in the mesopause region (87 km) from measurements made at Maimaga and Tiksi stations. These stations record spectra, using identical Shamrock photosensitive infrared spectrographs (manufactured by Andor Technology Ltd) detecting the OH (3, 1) band in the near-infrared region (~1.5 μm). We have analyzed data derived from the 2015–2017 observation seasons at Maimaga and Tiksi.

We have obtained standard temperature deviations corresponding to internal gravity waves (σ_{gw}) and tidal waves (σ_{td}). Mean night temperatures, tidal and IGW components are roughly the same for the two seasons of simultaneous observations at Tiksi and Maimaga. The seasonal variations in standard deviations caused by IGW and tidal waves recorded at Maimaga and Tiksi have been compared with those obtained at Wuppertal, Zvenigorod, and Tory.

This work was supported by NOFMU grant No. 20170220219 and RFBR grant No. 7-05-00855 A.

REFERENCES

Ammosov P.P., Gavrilyeva G.A. Infrared Digital Spectrograph for Measuring Hydroxyl Rotational Temperature. *Prib. Tekh. Eksp.* 2000, vol. 43, no. 6, pp. 792–797.

Baker D.J., Stair A.T. Rocket measurements of the altitude distributions of the hydroxyl airglow. *Physica Scripta.* 1988, vol. 37, pp. 611–622.

Brasseur G., Solomon S. *Aeronomiya srednei atmosfery* [Aeronomy of the middle atmosphere]. Leningrad, Gidrometeoizdat Publ., 1987. 413 p. (In Russian).

Chapman S., Lindzen R. *Atmosfernye prilivy* [Atmospheric tides]. Moscow, Mir Publ., 1972. 295 p. (In Russian).

Gavrilyeva G.A., Ammosov P.P. Seasonal variation in the mesopause temperature over Yakutsk (63° N, 129.5° E). *Geomagnetism and Aeronomy.* 2002, vol. 42, no. 2, pp. 267–271.

Goldman A., Schoenfeld W. G., Goorvitch D., Chackerian Jr.C., Dothe H., Mélen F., Abrams M.C., Selby J.E. A. Updated line parameters for OH $X^2\Pi$-$X^2\Pi$ (v″, v′) transitions. *J. Quantitative Spectroscopy and Radiative Transfer*. 1998, vol. 59, pp. 453–469.

Hines C.O. The upper atmosphere in motion. AGU. Washington D.C., 1974. 1027 p.

Mies F.H. Calculated vibrational transition probabilities of OH(X2Π). *J. Molecular Spectroscopy*. 1974, vol. 53, no. 2, pp. 150–180.

Noll S., Kausch W., Kimeswenger S., Unterguggenberger S., Jones A. M. OH populations and temperatures from simultaneous spectroscopic observations of 25 bands. *Atmospheric Chemistry and Physics.* 2015, vol. 15, pp. 3647–3669.

Offermann D., Gusev O., Donner M., Forbes J.M., Hagan M., Mlynczak M.G., Oberheide J., Preusse P., Schmidt H., Russell J.M. III. Relative intensities of middle atmosphere waves. *J. Geophys. Res.* 2009, vol. 114, p. D06110.

Offermann D., Hoffmann P., Knieling P., Koppmann R., Oberheide J. Long-term trends and solar cycle variations of mesospheric temperature and dynamics. *J. Geophys. Res.* 2010, vol. 115, p. D18127.

Offermann D., Wintel J., Kalicinsky C., Knieling P., Koppmann R., Steinbrecht W. Long-term development of short-period gravity waves in middle Europe. *J. Geophys. Res.* 2011, vol. 116, p. D00P07.

Perminov V.I., Medvedeva I.V., Semenov A.I. Temperature variability in the mesopause region from midlatitude measurements of the hydroxyl emission. *Sovremennye problemy distantsionnogo zondirovaniya Zermli iz kosmosa* [Current Problems in Remote Sensing of the Earth from Space]. 2013, vol. 10, no. 1, pp. 134–141. (In Russian).

Perminov V.I., Semenov A.I., Medvedeva I.V., Pertsev N.N. Temperature variations in the mesopause region according to the hydroxyl-emission observations at midlatitudes. *Geomagnetism and Aeronomy*. 2014, vol. 54, no. 2, pp. 230–239.

Shefov N.N., Semenov A.I., Khomich V.Yu. *Izuchenie verkhnei atmosfery — indikator ee struktury i dinamiki* [Research into the upper atmosphere as an indicator of its structure and dynamics]. Moscow, GEOS Publ., 2006. 741 p. (In Russian).

Takano M., Watanabe T., Nakamura M. Rocket measurements of O2 atmospheric (0-0) and OH Meinel bands in the night airglow. *J. Geomagn. Geoelectr.* 1990, vol. 42, pp. 1193–1208.

van der Loo M.P.J., Groenenboom G.C. Theoretical transition probabilities for the OH Meinel system. *J. Chem. Phys.* 2007, vol. 126, p. 114314.

Yee J.H., Growley G., Roble R.G., Skinner W.R., Burrage M.D., Hays P.B. Global simulations and observations of OI (^{1}S), O_2 ($^1\Sigma$), and OH mesospheric nightglow emissions. *J. Geophys. Res.* 1997, vol. 102, pp. 19949–19968.

Zhang S.P., Shepherd G.G. The influence of the diurnal tide on the O(1S) and OH emission rates observed by WINDII on UARS. *Geophys. Res. Lett.* 1999, vol. 26, p. 529.

How to cite this article

Sivtseva V.I., Ammosov P.P., Gavrilyeva G.A., Koltovskoi I.I., Ammosova A.M. Comparison between seasonal variations in tidal and internal gravity wave activity as derived from observations at Maimaga and Tiksi. *Solar-Terrestrial Physics*. 2018. vol. 4, iss. 2. pp. 69–72. DOI: 10.12737/stp-41201811